Soil Water Content Monitoring Using Electromagnetic Induction

Robert C. Reedy[1] and Bridget R. Scanlon[2]

Abstract: The use of electromagnetic (EM) induction measurements was evaluated to predict water content in the upper 1.50 m of a prototype engineered barrier soil profile designed for waste containment. Water content was monitored with a neutron probe, and bulk soil electrical conductivity was monitored with a Geonics EM38 ground conductivity meter at ten locations at approximately monthly intervals over a three-year period. A simple linear regression model accurately predicted average volumetric water content of the profile at any location at any time ($R^2=0.80,\sigma=0.009$) and spatially averaged volumetric water content over the entire area at any time ($R^2=0.99,\sigma=0.003$). Although some temporal drift was present in the model residual values, the impact on predicted water content was negligible. Therefore, once the model is calibrated with the neutron probe over a sufficient range of water contents, further neutron probe measurements may not be necessary. EM induction has several advantages over traditional water content monitoring techniques, including nonradioactivity, speed and ease of use over larger areas, and noninvasive character.

DOI: 10.1061/(ASCE)1090-0241(2003)129:11(1028)

CE Database subject headings: Soil water; Monitoring; Measuring instruments.

Introduction

Information on average water content in near-surface soils is important for assessing land atmosphere interactions, infiltration, deep percolation or recharge, water balance, and performance of engineered covers. Engineered covers are widely used to minimize water movement into underlying waste, including municipal solid waste, industrial waste, and hazardous waste (Daniel and Koerner 1995). They are also being proposed for many contaminated sites where remediation is technically infeasible (Wing and Gee 1994; Dwyer 2001). Thousands of sites are deploying engineered covers throughout the United States that may extend over large areas (hectares). Measurement of water content or water storage in the cover soils is used to assess the performance of the covers (Ward and Gee 1997). Water content data are also required to validate water balance models of near-surface soils using codes such as *UNSATH* (Fayer et al. 1992; Khire et al. 1997; Scanlon et al. 2003). Subsidence or desiccation of engineered covers may result in localized areas of increased water content, in turn resulting in potential performance failure. Information on water content at specific locations is therefore required.

Conventional techniques for measuring and monitoring water content include destructive soil sampling and oven drying, neutron thermalization, and time domain reflectometry (Gardner 1986; Dalton 1992). As these techniques generally measure water content at a particular point, it is costly and time consuming to monitor large areas using them.

Electromagnetic (EM) induction can also be used to estimate soil water content. Bulk soil electrical conductivity (EC) generally varies with clay content, water content, and salinity (McNeill 1980). EM induction is a noninvasive technique that measures a depth-weighted average of EC, termed the apparent electrical conductivity (EC_a). Previous studies have shown that the controlling factor in some areas is clay content (Cook and Walker 1992), salinity (Rhoades et al. 1990; Lesch et al. 1995), and water content (Kachanoski et al. 1988, 1990; Sheets and Hendrickx 1995) and can include all three factors in different parts of a study area (Paine et al. 1998; Scanlon et al. 1999). Kachanoski et al. (1988) found that EC_a explained 96% of the spatial variation in water content in the upper 0.5 m of the profile of a 1.8-ha field. In another study, Kachanoski et al. (1990) compared water content monitored with neutron probes installed at 10-m intervals along a 660-m transect with EC_a monitored with EM31 and EM38 meters (Geonics Inc., Mississauga, Canada). Values of EC_a and water content were not correlated at scales <40 m; however, at scales $\geqslant 40$ m, EC_a explained more than 80% of the variation in water content. Sheets and Hendrickx (1995) conducted a similar study that used 65 neutron probe access tubes at 30-m intervals and compared water content measurements with EC_a readings using an EM31 meter for 16 monthly measurements. The lower R^2 (0.64) calculated for this study relative to that calculated by Kachanoski et al. (1988, 1990) was attributed to the deeper penetration of the EM31 meter (4 m) relative to the water content monitoring (1.50 m) and the distance between the EM measurements and the neutron probe access tubes (10 m). The correlation was improved by using monthly calibrations, and a residual standard deviation of 0.019 was obtained for the 1.5-m soil profile.

The purpose of this study was to evaluate the use of EM induction to monitor average water content and changes in water content in the upper 1.5 m of the soil profile at point locations and over an area of an engineered soil cover. The main difference

[1]Bureau of Economic Geology, Jackson School of Geosciences, The Univ. of Texas at Austin, Univ. Station, Box X, Austin, TX 78713-8924.

[2]Bureau of Economic Geology, Jackson School of Geosciences, The Univ. of Texas at Austin, Univ. Station, Box X, Austin, TX 78713-8924. E-mail: Bridget.Scanlon@beg.utexas.edu

Note. Discussion open until April 1, 2004. Separate discussions must be submitted for individual papers. To extend the closing date by one month, a written request must be filed with the ASCE Managing Editor. The manuscript for this paper was submitted for review and possible publication on March 8, 2002; approved on January 22, 2003. This paper is part of the ***Journal of Geotechnical and Geoenvironmental Engineering***, Vol. 129, No. 11, November 1, 2003. ©ASCE, ISSN 1090-0241/2003/11-1028–1039/$18.00.

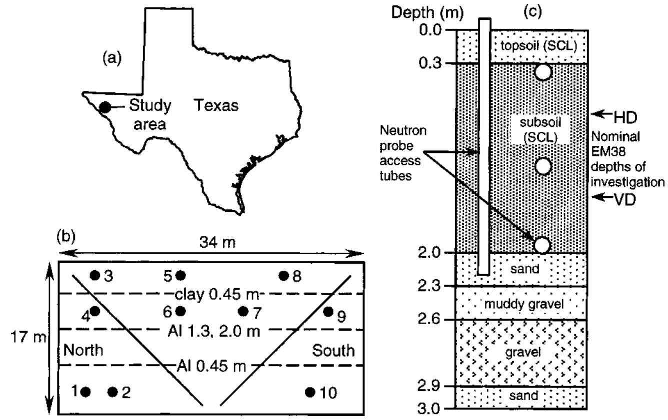

Fig. 1. (a) Study area location. (b) Relative positions of vertical (solid symbols) and horizontal (dashed lines) neutron probe access tubes, and soil sample transects (solid diagonal lines). Horizontal access tube designations indicate pipe material (Al: aluminum) and depth(s) of burial. (c) Engineered cover cross section (SCL: sandy clay loam; HD: horizontal dipole mode; VD: vertical dipole mode).

between this and previous studies is that this study includes detailed evaluation of spatial and temporal variability in water content, whereas other studies focus only on spatial variability in water content (Kachanoski et al. 1988, 1990). This study also should provide a more accurate evaluation of the use of EM induction than that provided by Sheets and Hendrickx (1995) because the EM38 meter is more appropriate for monitoring water content in the upper 1.5 m and EM readings were conducted at the location of the neutron probe measurements.

Materials and Methods

The study area is located approximately 145 km southeast of El Paso, Tex., in the Chihuahuan Desert [Fig. 1(a)]. Water content and EM measurements were conducted on the upper 2 m of an engineered cover. The engineered cover was constructed with soils obtained from a nearby excavation at depths from 0 to 10 m. The dimensions of the engineered cover are 34 m×17 m [Fig. 1(b)]. The soils in the engineered cover consisted of sandy clay loam in the upper 2 m [Fig. 1(c)]. The dry bulk density of the cover topsoil (0- to 0.3-m depth) was 1,500 kg/m^3, whereas the cover subsoil (0.3- to 2.0-m depth) was compacted to 1,800 kg/m^3.

Soil Salinity and Clay Content Measurements

Soil samples were collected during site construction at 14 locations along two transects and analyzed for texture and salinity [Fig. 1(c)]. Vertical profiles were equally spaced at 3.0-m intervals, and samples were taken at 0.3-m-depth intervals to a depth of 1.8 m. A total of 84 samples were analyzed for saturated paste conductivity (EC_p), saturation percentage of the soil paste, and percent sand, silt, and clay following Anonymous (1954). Estimates of the saturated paste extract conductivity (EC_e) were calculated following Rhoades (1992).

Water Content Measurements

Water content was monitored with a neutron probe in 10 PVC neutron probe access tubes from July 1998 through July 2001 [Fig. 1(b)]. The access tubes were installed to an average depth of 2.2 m and were irregularly spaced to avoid metallic instrument cables, conduits, and horizontal neutron probe access tubes buried at several depths and locations within the cover. The neutron probe was calibrated using 35 core samples obtained during installation of the access tubes, and volumetric water content θ in the core samples ranged from 0.047 to 0.226. A linear regression calibration model of neutron counts versus volumetric water content resulted in R^2 of 0.96 and a residual standard deviation of 0.011. Water content was monitored at 0.15-m intervals to a depth of 2.10 m. A neutron count measurement duration of 64 s was used in this study and resulted in an average neutron count precision of ±0.74% (range from ±0.62% to ±1.20%) for all measurements, translating to an average volumetric water content measurement precision of ±0.0019 (range from ±0.0016 to ±0.0030). Neutron probe surveys of all ten locations required approximately 3 h to complete.

No separate calibration was performed for the 0.15-m depth. Neutron counts for the 0.15-m-depth measurements were adjusted using a correction factor to account for the loss of neutrons at the soil surface (Greacen et al. 1981, *after* Grant 1975). The correction factor was calculated from

$$\log(C-1) = -0.855 \log \theta - 1.8446 \tag{1}$$

where C = correction factor; and θ = volumetric water content at a depth of 0.15 m. Measured neutron counts were multiplied by an initial estimate of C to calculate an initial estimate of θ using the calibration model. The initial estimate of θ was substituted into Eq. (1), and a refined estimate of C was calculated. The measured neutron counts then were multiplied by the refined estimate of C to calculate a new estimate of θ. The process was reiterated until successive changes in C were <0.001. Average correction factors between different locations ranged from 1.048 to 1.104 for different measurement times. Multiplying the neutron probe counts by the correction factors resulted in an upward adjustment of the average volumetric water content at the 0.15-m depth that ranged from 0.012 to 0.016 for different measurement times.

The average water content at each location was calculated for depth intervals from 0 to 0.75 m (θ_{75}) and from 0 to 1.50 m (θ_{150}) by integration of the water content measurements. The spatially averaged water content over a given depth interval for a given survey date was calculated as the simple arithmetic average of the measurements from each access tube location. Spatially averaged water content values were not weighted on the basis of the irregular access tube spacing.

Water content was also measured in four horizontal neutron probe access tubes installed during site construction [Fig. 1(b)]. One of the horizontal access tubes was constructed of 0.152-m-diameter (6-in.) clay pipe installed at 0.45-m depth, and the remaining three tubes were constructed of 0.102-m (4-in.) aluminum pipe installed at 0.45-, 1.2-, and 2.0-m depths [Fig. 1(b)]. Six surveys were conducted on the horizontal access tubes at irregular time intervals between March 1998 and November 2000. Approximately 110 measurements were obtained at 0.3-m intervals at each depth across the length of the installation. Calibrations were generated by transference of the vertical access tube measurements to the nearest locations in the horizontal access tubes. A linear regression calibration model of volumetric water contents ranging from 0.169 to 0.241 for the clay access tube resulted in an R^2 of 0.99 (residual $\sigma = 0.003$). The calibration for the aluminum access tubes resulted in an R^2 of 0.82 (residual $\sigma = 0.007$) over approximately the same water content range. The clay access tube was more closely spaced to a greater number of vertical access tubes than were the aluminum tubes, resulting in the higher R^2 value.

Apparent Electrical Conductivity Measurements

EM induction measurements were made with the Geonics EM38 ground conductivity meter. The EM38 instrument response is a nonlinear, depth-weighted measurement of apparent soil bulk conductivity (EC_a). The EM38 has an intercoil spacing of 1.0 m with a nominal depth of investigation, defined as the depth to which approximately 70% of the measured response is generated, of 1.50 m when operated in the vertical dipole (VD) mode and 0.75 m when operated in the horizontal dipole (HD) mode (McNeill 1980). The VD mode response is less sensitive than the HD response to near surface material ($<\sim$0.40-m depth) and more sensitive to deeper material.

A total of 35 surveys were conducted between July 1998 and July 2001 at a median time interval of 32 days, ranging from 7 to 71 days. Measurements of EC_a were performed at the same times as the water content measurements. The EM38 was operated to obtain both VD and HD readings, with the instrument on the ground immediately adjacent to the vertical neutron probe access tubes. The EM38 instrument zero and in-phase null were calibrated at each location prior to data collection. Complete surveys of all ten locations were performed in approximately 15 min.

Soil temperature correction of EC_a values is essential (McKenzie et al. 1989). Average soil temperature at the site ranged from 8 to 31°C over different depth intervals at different times, requiring the EC_a to be standardized to allow a comparison between values monitored at different times. Soil temperature was measured using thermistors (± 0.1°C) installed at seven depths ranging from 0.15 to 2.00 m. Average soil temperature values were determined for the 0 to 0.75-m and 0 to 1.50-m depth intervals by vertical integration of the temperature data. Apparent electrical conductivity measurements were standardized to 25°C using

$$EC_{25} = EC_a(0.4779 + 1.3801e^{(-T/25.654)}) \tag{2}$$

where EC_{25} = temperature-standardized; EC_a and T(°C) = average temperature over a given depth interval. Eq. (2) was developed through regression of tabulated data for the 3 to 35°C range (Anonymous 1954). Correction factors [term in parenthesis in Eq. (2)] ranged from 0.90 during warmer months to 1.47 during colder months. The average temperatures in the top 0.75 and 1.50 m were used to calculate temperature-standardized HD readings (EC_H) and VD readings (EC_V), respectively.

Data Analysis and Model Development

Measured water content data were examined for spatial and temporal correlation. The spatial correlation of water contents measured in the horizontal access tubes was examined using variograms (Pannatier 1996). There were insufficient data for a temporal analysis of the horizontal access tube data. With only ten measurement points per survey in the vertical access tubes, spatial variograms for a given survey date were noisy. Accordingly, descriptive statistics of the temporal variability of measured water content for each of the ten locations were summarized and compared using percentile box plots.

The relationships between measured water content and EC_{25} were investigated using analysis of covariance (ANOCOVA). Analysis of covariance is a technique that combines the features of analysis of variance and regression (Snedecor and Cochran 1967). Simple ANOCOVA models were initially developed that incorporated only the EC_{25} measurements (EC_V and EC_H) and a parameter to adjust for any temporal effects. The simple models were used to determine which combination of EC_V and EC_H measurements provided the best predictions of water content. The resulting preferred model was then reformulated to formally test for both spatial and temporal effects using a more rigorous ANOCOVA analysis. The formal models included parameters to examine the relative contributions (i.e., significance) of both location and time to the variability in the relationship between measured water content and EC_{25}. Last, simple linear regression models were developed for the relationship between measured water content and EC_{25}. The residual water contents at each location were examined for temporal trends (i.e., first-order autocorrelation).

Simple ANOCOVA models were used to evaluate the relationships between the measured water content over each depth interval with the EC_H and EC_V measurements. Three linear combinations of the measurements are possible; therefore, three model parametrizations were initially investigated

$$\theta_{y,t} = a + b(EC_H) + c(EC_{(V-H)}) + d_t(\text{Time}) \tag{3a}$$

$$\theta_{y,t} = a + b(EC_H) + d_t(\text{Time}) \tag{3b}$$

$$\theta_{y,t} = a + b(EC_V) + d_t(\text{Time}) \tag{3c}$$

where θ = vertically integrated volumetric water content; subscript y = depth interval (0–0.75 m or 0–1.50 m); and subscript t = monitoring times ($t = 1-35$). The subscript $(V-H)$ = difference between EC_V and EC_H. The difference was used rather than EC_V alone because of the strong correlation between EC_V and EC_H readings ($R^2 = 0.83$). Time was included in each parameterization as a discrete, fixed effect to adjust for possible temporal bias in the model coefficients. Based on the analysis results described subsequently, Model (3*b*) was selected as the preferred model.

A more comprehensive ANOCOVA model then was used to formally test Model (3*b*) for both spatial and temporal effects. The model incorporated multiple parameters to characterize the effects of both location and time. Eq. (4) was used with both water content data sets (0 to 0.75-m and 0 to 1.50-m depth data)

$$\theta_{ij} = a + \beta(EC_H) + \alpha_1(\text{Site}) + \alpha_i\beta(\text{Site*}EC_H) + \delta_j(\text{Time}) + \delta_j\beta(\text{Time*}EC_H) + \varepsilon_{ij} \tag{4}$$

with $i = 1,2,\ldots,10$ locations and $j = 1,2,\ldots,35$ monitoring times. In Eq. (4), Site was treated as a random effect and assumed to be spatially independent. The statistical significance of β (the main EC_H slope estimate) was tested using the (Site*EC_H) interaction effect. Time was treated as a fixed effect and used to adjust for temporal trends in the data and also to help neutralize any temporal correlation in the residual water contents. The (Time*EC_H) interaction term was used to test for the stability of the β parameter over time.

The relative statistical significances of the various interactions at each of the ten locations over the 35 monitoring times were quantified using the F-test statistics and associated p values for each model parameter. The p value is inversely proportional to parameter significance and represents the probability that the observed effect of a given parameter is the result of random chance. Thus, smaller values of p indicate greater significance.

Simple linear regression models were fitted to all 350 observations [Eq. (3*b*), excluding the Time parameter], and the resulting model residuals were directly analyzed for both spatial and temporal correlation. Percentile box plots were used to summarize the degree of non-random spatial variation. The residuals at individual locations and the average residuals for each monitoring time were analyzed for temporal trends and other evidence of nonstationary behavior. All regression and statistical analyses were performed using *SAS version 8.02* software (SAS Institute, Cary, North Carolina). Volumetric units (m^3/m^3) were used to compare water content predictions over different depth intervals.

Clay content, salinity, and water content are factors that affect bulk electrical conductivity. The relative contributions (resulting from the spatial variability at our site) of each of these factors to the spatial variability of EC were estimated through time. Estimates of EC were calculated following Rhoades (1992) using the clay content and EC_e data from the sampled transects and the measured water content values at each monitoring location and time. The approach used assumes that the mean and standard deviation values of clay content and salinity at the sampled locations are representative of the values at the water monitoring locations. The relative contribution of each factor to the spatial variability of EC was estimated by maintaining a constant (average) value for that factor while allowing the remaining factors to vary over the observed ranges. The (spatial) coefficient of variation (CV) of estimated EC was used to compare the relative contributions of clay content, salinity, and water content.

The contribution of clay content to spatial variability in EC was estimated by maintaining both EC_e and water content constant at the spatial average value for each depth. The measured clay content values were used and values of EC were calculated for each of the 14 sampled locations as the average of the individual depth estimates at each location for each monitoring time. The EC CV due to spatial variation in clay content was calculated for each monitoring time. The contribution of salinity to the spatial variability of EC was similarly estimated by maintaining both clay content and water content constant at the average value for each depth. Finally, the contribution of water content to the spatial variability of EC was estimated by maintaining both clay content and EC_e constant at their spatial average values for each depth. The water content profiles at the ten monitored locations were used and estimates of EC were calculated for each location as the average of the individual depth estimates, resulting in ten values for each monitoring time. The EC CV due to spatial variation in water content was calculated for each monitoring time.

Results and Discussion

Spatial Variability of Clay Content and Salinity

Results of the textural and salinity analyses are summarized in Fig. 2. The soils in the upper 1.8 m of the cover were texturally uniform (topsoil: 51±6% sand, 27±3% silt, and 22±3% clay; subsoil: 55±3% sand, 21±2% silt, and 24±2% clay). Clay content was generally uniform at a given location and across locations at a given depth. Vertically averaged clay content (i.e., the average of clay content values at a given location) was spatially uniform with a CV of 4%. Across locations at different depths, average clay content ranged from 22 to 25% and standard deviations ranged from 1 to 3% (CV range: 5–12%). Compared to clay content, vertically averaged EC_e was more spatially variable with a CV of 12%. Across locations at different depths, average EC_e ranged from of 5.1 to 5.6 dS/m to a depth of 1.50 m and was 2.7 dS/m at the 1.80-m depth. EC_e was more spatially variable at a given depth than clay content, with standard deviations ranging from 1.0 to 1.8 dS/m (CV range: 19–36%) to the 1.50-m depth and 0.5 dS/m (CV=19%) at the 1.80-m depth.

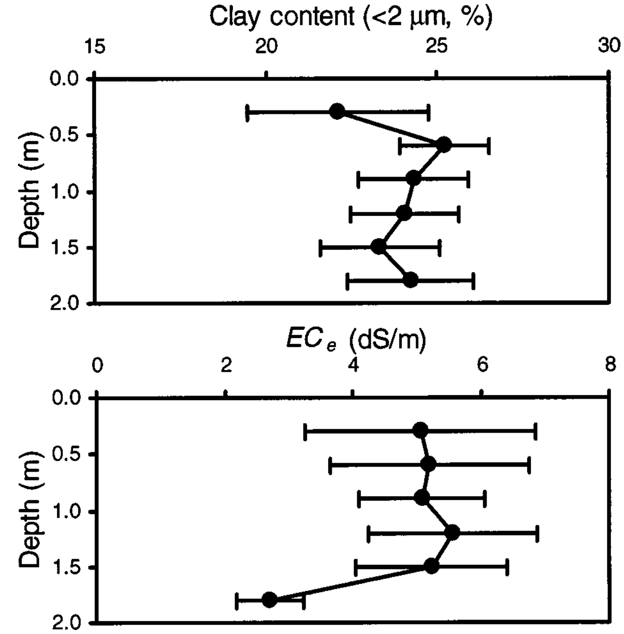

Fig. 2. Average clay content and saturated paste extract conductivity (EC_e) with depth (six depths, $n=14$ at each depth). Error bars represent one standard deviation.

Spatial and Temporal Variability of Water Content Measured with the Neutron Probe

Both spatial and temporal variability of water content were greater over the 0- to 0.75-m-depth interval than over the 0- to 1.50-m-depth interval [Fig. 3(a)]. Volumetric water content at the ten measurement locations was generally more spatially variable at a given time in the 0- to 0.75-m-depth interval (average $\sigma=0.012$) than in the 0- to 1.50-m depth interval (average $\sigma=0.008$) (Table 1). Average water content increased with depth throughout most of the study period, as shown by the higher water content in the 0- to 1.50-m zone relative to that in the 0- to 0.75-m zone. Temporal variability in water content was characterized by an initial increase in water content in response to irrigation and precipitation, followed by a long-term drying trend and then fairly uniform conditions punctuated by short-term increases in water content in response to precipitation. Spatial variability of measured (vertically averaged) water content (CV=4%) was similar to that of clay content (CV=4%) and less than that of EC_e (CV=12%).

The horizontal access tube surveys indicated that, at a given time, volumetric water contents were generally within ±0.01 (1,σ) of the average at a given depth across the test area. For each of the horizontal access tube surveys, the water content measurements at similar lateral offset distances were averaged across all access tube depths (0.45, 1.2, and 2.0 m). The resulting one-dimensional data sets provided approximations of the vertically averaged water content at 0.3-m intervals across the length of the study area. The variograms for each survey date showed a consistent pattern, indicating that the lateral correlation range of vertically averaged water content was less than ~2 m (Fig. 4). The variograms also showed an oscillation with a wavelength of from 4 to 5 m. The reason for the oscillation is unclear but may be

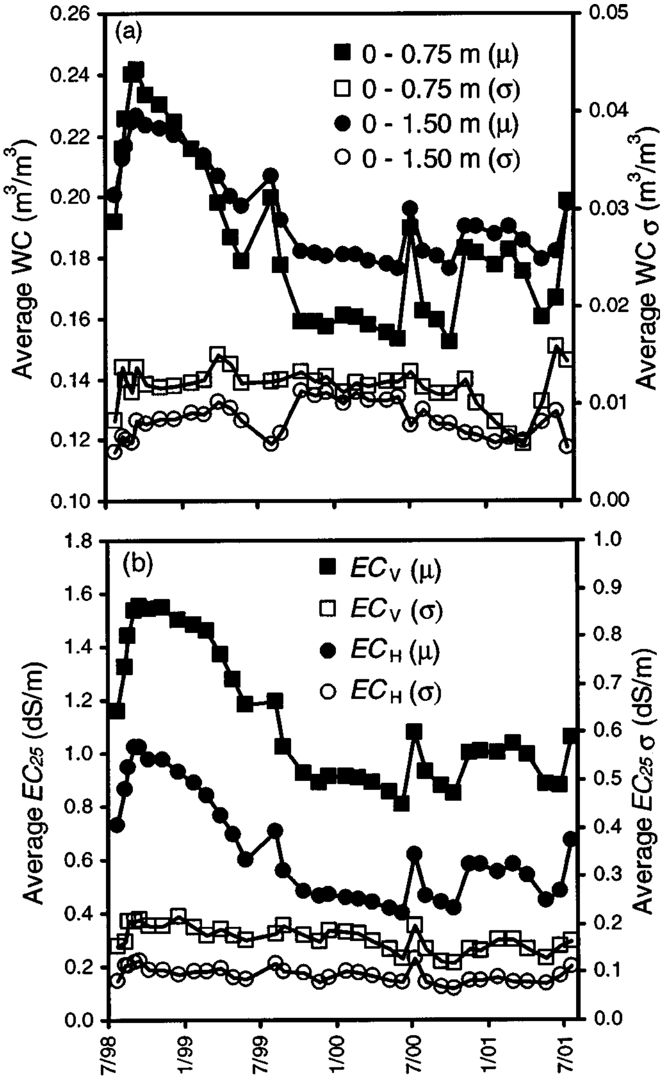

Fig. 3. Variation in (a) neutron probe average water content (WC) and standard deviation (σ) for different depth intervals and (b) EC_V and EC_H average and σ values. Average values are based on ten measurement locations.

related to small differences in soil compaction around the locations of other instrument systems that have lateral offsets of 4 to 6 m and that are located near the horizontal access tubes.

The vertical access tubes appeared to be sufficiently distant from one another to be considered spatially independent with regard to the water content spatial correlation structure observed in the horizontal access tubes. The smallest separation distance was 3 m between Locations 1 and 2, whereas other separation distances ranged from 4 to 28.5 m. Percentile box plots depicting the temporal distribution of water content measurements at each location indicated a slight southerly trend toward lower average volumetric water contents (Fig. 5), and for both depth intervals the magnitude of the trend was approximately 0.01. The southerly locations were also more variable through time than the northerly locations. The spatial trend and the greater temporal variability at the southerly locations are consistent with the observed distribution of vegetation, which was denser in the south half of the facility. However, all temporal average water contents between nearby locations were the same at the 95% confidence level. Most of the mean 95% confidence intervals at individual locations overlapped with those at other locations. The only exceptions were between locations with the greatest separation distances [e.g., Locations 1 and 9, Fig. 1(b)].

Table 1. Measured Water Contents in 0- to 0.75-m and 0- to 1.50-m Depth Intervals

Interval (m)	θ Range[a] (m³/m³)	σ Average[b] (m³/m³)	σ Range[c] (m³/m³)
0–0.75	0.152–0.241	0.012	0.006–0.016
0–1.50	0.176–0.227	0.008	0.005–0.011

[a]Range of measured water contents averaged over the ten measurement locations for the 35 surveys.

[b]Average of all 35 survey σ values, each with $n=10$ (representing the ten measurement locations).

[c]Range of average σ values over the 35 surveys.

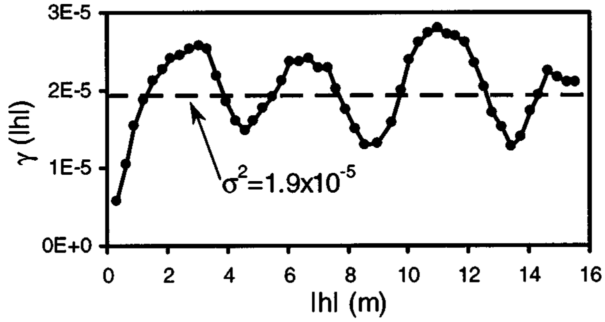

Fig. 4. Semivariogram (γ) of combined horizontal neutron probe access tube water content measurements for the November 2000 survey (lag$=0.31$ m); h is the (absolute) separation distance; σ^2 is the data variance ($n=110$). A spherical model was fitted to the data with range$=1.5$ m, sill$=\sigma^2$, and nugget$=2.0\times10^{-6}$.

Visual comparison between Figs. 3(a and b) indicates that the trends in EC_{25} for both horizontal and vertical dipole modes followed the trends in measured water content through time. EC_V was consistently greater in magnitude than EC_H, indicating that soil bulk conductivity increased with depth (Table 2).

Preferred Model for Predicting Water Content

The regressions showed that Eqs. (3*a*) and (3*b*) produced nearly equivalent results and both were more accurate (higher R^2 and lower residual σ) than model 3c (Table 3). A preliminary test of the coefficients of Eq. (3*a*) revealed that the *c* coefficient was not significantly different from zero at the $\alpha=0.01$ confidence level. Additionally, the lack of any substantial improvement in the R^2 (and/or reduction in the standard error estimate) suggested that the EC_{V-H} term could be omitted from the model. As a result, Eq. (3*b*) was selected as the preferred model parametrization.

Interestingly, the EC_H models based on Eq. (3*b*) consistently generated better predictions of water content and had greater significance than did the EC_V models based on Eq. (3*c*) (Table 3). The higher correlations and lower residual standard deviations of the EC_H models relative to the corresponding EC_V models may be explained by the contrast between the HD and VD relative response functions with depth for the EM38 instrument (Fig. 6). Most of the spatial and temporal changes in water content occurred nearer the surface at depths where a greater percentage of the total HD response was generated relative to the total VD response. Approximately 73% of the combined spatial and temporal variability in water content over the 0- to 2.1-m-depth interval occurred in the top 0.75 m, and 90% occurred in the top

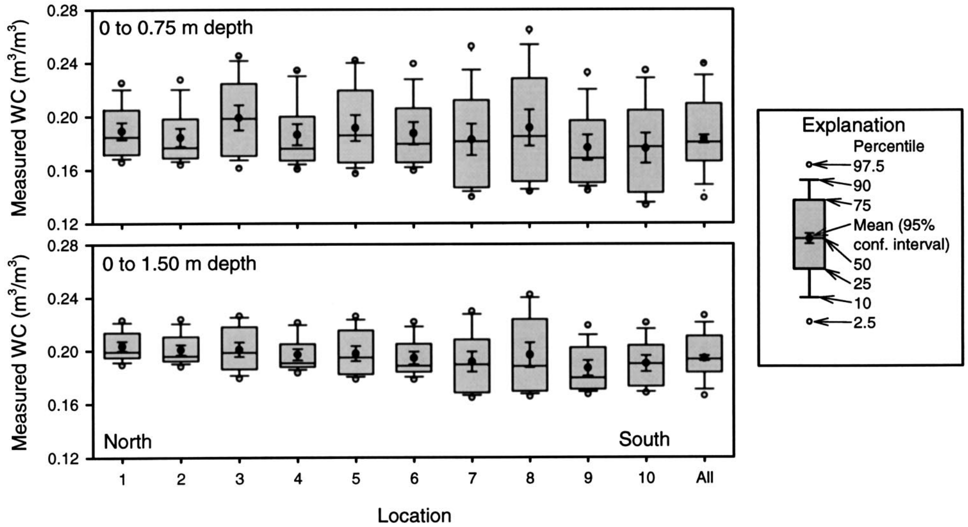

Fig. 5. Percentile box plots of water content (WC) measured with the neutron probe in the different depth intervals at each of the ten monitored locations ($n=35$). Locations 1 through 10 generally indicate northerly to southerly locations [Fig. 1(b)]. "All" locations represent the pooled values for each depth interval ($n=350$).

1.50 m. Over the same depth intervals, respectively, 70 and 84% of the HD response is generated compared with only 45 and 68% of the VD response.

Analysis of Covariance

Results for the rigorous θ_{75} ANOCOVA model are shown in Table 4. The model produced an overall R^2 value of 0.96, and a volumetric water content root mean square error (RMSE) of 0.0071. The F-test associated with the main EC_H slope term was highly significant (small p), suggesting that the temperature corrected HD signal data were strongly correlated with the measured 0- to 0.75-m-depth water contents. The EC_H*Time interaction effect was not significant (large p), suggesting that the slope term is stable over time. However, the Time effect was statistically significant, implying that the average prediction error changed systematically over time. Additionally, although both the Site and EC_H*Site interaction terms were considered random effects in this ANOCOVA model, their associated high F-test values suggest that there is a significant location effect within the conductivity/water content relationship. Overall, the sequential sum of squares results indicate that 87.3% of the total θ_{75} variability is explained by the main EC_H slope term, 10.1% of additional variation is explained by location effects (the Site and EC_H*Site terms), and another 2.6% of the total variation is related to temporal effects.

Results for the rigorous θ_{150} ANOCOVA model are shown in Table 5. This second model also produced an overall R^2 value of 0.96, and a volumetric water content RMSE of 0.0043. The individual parameter F-test results were basically the same as for the θ_{75} model. The F-test associated with the main EC_H slope term was highly significant. The EC_H*Time interaction effect was not significant. The Time effect was statistically significant, and high F-test values were observed for both the Site and EC_H*Site interaction terms. In this second model, the sequential sum of squares results indicate that 83.1% of the total θ_{150} variability is explained by the main EC_H slope term, 14.4% of additional variation is explained by location effects (the Site and EC_H*Site terms), and another 2.6% of the total variation is related to temporal effects.

The results from these two analyses indicate that the EC_H data effectively account for the predominant variation in water content. However, additional spatial and temporal effects are also present in the data, which may need to be accounted for. These latter effects are important to quantify, because a much more limited amount of calibration data would probably be collected in an actual water content monitoring application and a much simpler calibration model might likely be employed.

Table 2. Measured Electromagnetic Response Values

Measurement	Range[a] (dS/m)	σ Average[b] (dS/m)	σ Range[c] (dS/m)
EC_H	0.40–1.02	0.095	0.064–0.132
EC_V	0.81–1.55	0.172	0.116–0.216

Note: Subscripts H and V represent horizontal and vertical dipole mode, respectively. All EC values are corrected to 25°C.

[a]Range of measured EC values averaged over the ten measurement locations for the 35 surveys.

[b]Average of all 35 survey σ values, each with $n=10$.

[c]Range of average σ over 35 surveys.

Table 3. Regression Analysis Results for Different Model Parametrizations

	0–0.75 m			0–1.50 m			Degrees of freedom	
Model	R^2	σ (m^3/m^3)	F	R^2	σ (m^3/m^3)	F	Model	Error
3a	0.892	0.0098	71.8	0.846	0.0071	47.8	36	313
3b	0.892	0.0098	73.7	0.842	0.0072	47.8	35	314
3c	0.869	0.0106	59.5	0.812	0.0078	38.7	35	314

Note: Models numbers refer to equations in text. All F values are significant to $p<0.0001$.

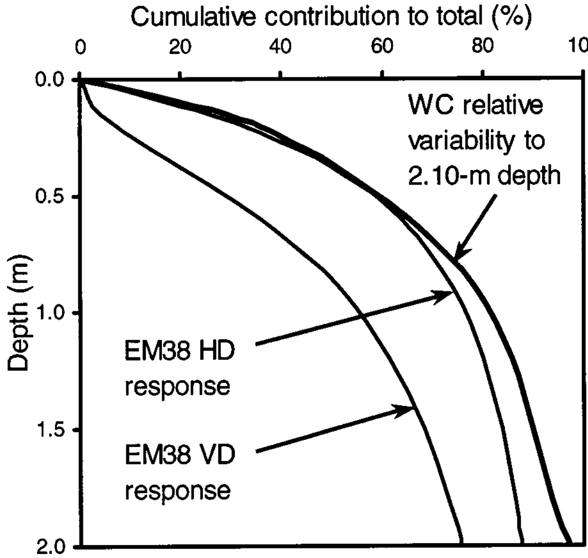

Fig. 6. Cumulative EM38 signal responses and relative temporal variability of average measured water content (WC) with depth. Curves for the horizontal dipole mode (HD) and vertical dipole mode (VD) were calculated from McNeill (1980) Eqs. (13) and (14) with an intercoil spacing of 1 m. Relative temporal variability was calculated from the standard deviations of the average measured water contents at each depth over the 35 monitoring times.

Direct Analysis of Model Residual Spatial Correlation

Additional analyses were performed to investigate the apparent spatial and temporal influences indicated by the rigorous ANOCOVA analyses. First, Eq. (3*b*) was simplified by omitting the Time term

$$\theta_y = a + b(\mathrm{EC}_H) \tag{5}$$

Kolmogorov-Smirnov distribution tests showed that the residuals for the two depth intervals modeled using Eq. (4) were normally distributed at the 95% confidence level (Fig. 7). On a volumetric basis, water contents over the 0- to 1.50-m depth were more accurately predicted than over the 0- to 0.75-m depth (Table 6).

The spatial variability of the regression model residuals for Eq. (5) was summarized using box plots by location (Fig. 8). Distinct spatial differences between the mean residual water contents are apparent across locations. However, these effects do not seem to clearly indicate spatial correlation. Indeed, Locations 1 and 2 represent the closest pair of neutron probes, yet their respective mean residual deviations are biased in opposite directions. Overall, the deviation in mean residual water contents seems to show little relationship to physical location. Additionally, the differences between locations are relatively small compared with the ranges in volumetric water content observed during the study period, and 98% of all predicted values at individual locations are within ± 0.02 of the measured values for the 0- to 1.50-m-depth interval.

Table 4. ANOCOVA Model Results for Water Content in 0- to 0.75-m Depth Interval

Parameter	Degrees of freedom	Mean square	Sequential sum of squares[a]	F	p
Overall	87	—	—	67.4	<0.0001
$\mathrm{EC_H}$	1	0.2575	0.873	5119.14	<0.0001
Site	9	0.0226	0.077	49.90	<0.0001
$\mathrm{EC_H}$*Site	9	0.0072	0.024	15.94	<0.0001
Time	34	0.0062	0.021	3.64	<0.0001
$\mathrm{EC_H}$*Time	34	0.0015	0.005	0.86	0.6916

Note: Overall model θ_{75} mean=0.186, R^2=0.96, root mean square error=0.0071, error degrees of freedom=262.

[a]Sequential sum of squares (calculated as the mean square divided by the sum of mean squares, 0.2950).

Table 5. ANOCOVA Model Results for Water Content in 0- to 1.50-m Depth Interval

Parameter	Degrees of freedom	Mean square	Sequential sum of squares[a]	F	p
Overall	87	—	—	68.8	<0.0001
$\mathrm{EC_H}$	1	0.0904	0.831	4975.57	<0.0001
Site	9	0.0113	0.104	68.84	<0.0001
$\mathrm{EC_H}$*Site	9	0.0043	0.040	26.36	<0.0001
Time	34	0.0022	0.020	3.50	<0.0001
$\mathrm{EC_H}$*Time	34	0.0006	0.006	0.95	0.5529

Note: Overall model θ_{150} mean=0.196, R^2=0.96, root mean square error=0.0043, error degrees of freedom=262.

[a]Sequential sum of squares (calculated as the mean square divided by the sum of mean squares, 0.1087).

Direct Analysis of Model Residual Temporal Correlation

To further characterize the temporal variability of model residuals, the mean residual water contents and residual standard deviations were calculated for each of the 35 monitoring times. Fig. 9 shows the apparent temporal patterns for both the 0- to 0.75-m

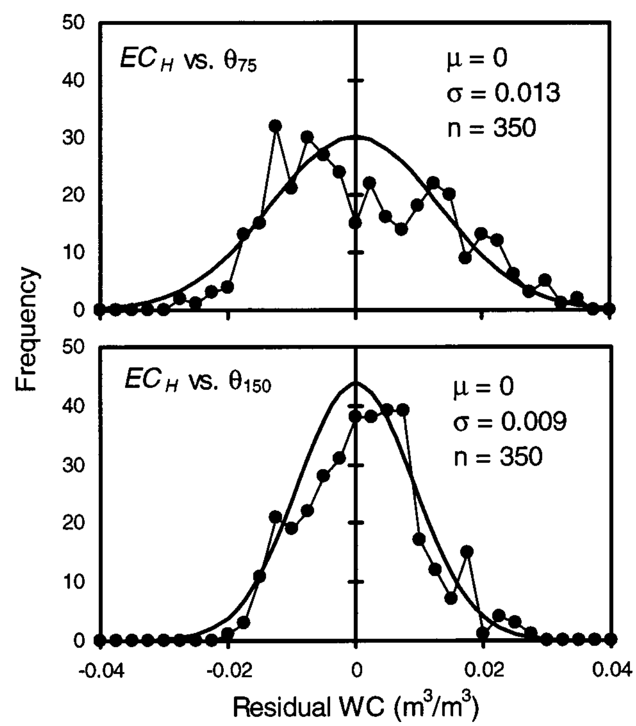

Fig. 7. Distribution of model residual water contents for the $[\theta_y = a + b(\mathrm{EC}_H)]$ models fit to the complete data sets (n=350). Smooth lines represent normal distribution functions with given average (μ) and standard deviation (σ) values.

Table 6. Regression Analysis Results for Model $[\theta_y = a + b(EC_H)]$ with $n = 350$

Depth interval (m)	a ($\times 10^2$) (m^3/m^3)	b ($\times 10^2$) ($m^3/m^3/dS$)	R^2	σ (m^3/m^3)
0–0.75	10.67±0.20	12.38±0.29	0.84	0.013
0–1.50	14.87±0.13	7.34±0.20	0.80	0.009

Note: Intercept (a) and slope (b) values are shown with respective standard errors.

and 0- to 1.50-m depths. The average residual volumetric water content for the 0- to 0.75-m depth displayed a generally consistent temporal trend with values ranging from approximately 0.005 at the beginning of the study to −0.005 at the end. Values for the 0- to 1.50-m depth also displayed a consistent temporal trend of approximately the same magnitude, but only during the first year of the study. After the first year, average residual water content values for the 0- to 1.50-m-depth remained close to zero.

We evaluated the correlation of the model residuals independently at individual locations through time and statistically significant temporal variation (first-order autocorrelation) was detected in the residual distributions. For the 0- to 0.75-m data, the apparent degree of first-order autocorrelation ranged from 0.081 to 0.639, with an average value of $r = 0.378$ across all ten locations. For the 0- to 1.50-m data, the first-order autocorrelation levels ranged from 0.116 to 0.804, with an average value of $r = 0.459$. Although not excessively high, these values confirm that some degree of temporal residual correlation exists in both data sets. In turn, this implies that, in an actual monitoring study, this temporal residual correlation pattern may need to be modeled, assuming water content data are collected over multiple times. Estimating the degree of residual correlation is important, because the temporal correlation structure can substantially impact the calculation of both the model mean square error term and the associated standard error estimates for comparing changes in water content over time. Conversely, if data from only one time are collected, then some assumptions about the degree of temporal correlation might need to be made. Though minor in this case, the primary cause of the noted temporal trends is likely changing

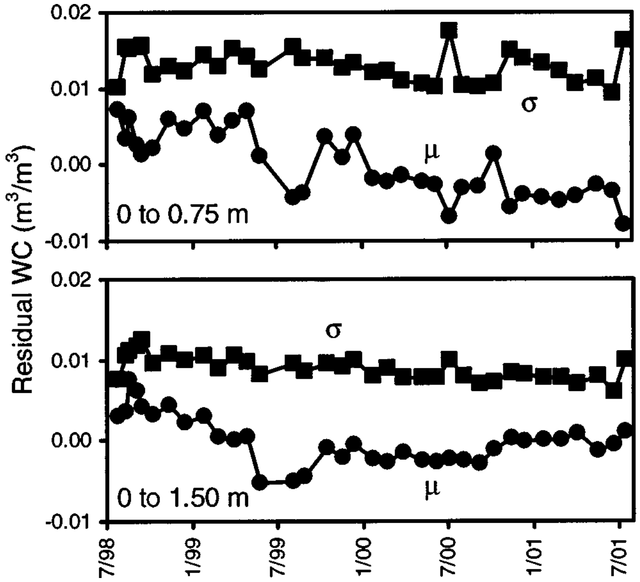

Fig. 9. Average residual water content (μ) and standard deviation (σ) ($n = 10$) through time for the $[\theta_y = a + b(EC_H)]$ models fit to the complete data sets ($n = 350$).

salinity with depth as water infiltrates. The analyzed samples were obtained prior to the onset of irrigation and some vertical redistribution likely occurred during and following irrigation.

Although statistically significant, the actual impacts of the temporal trends on water content predictions were small in practical terms. Over the course of the three-year study period, the overall residual trend rate was -0.0037 m^3/m^3/year for the 0- to 0.75-m depth (Fig. 9). The overall residual trend rate for the 0- to 1.50-m depth was -0.0016 m^3/m^3/year, though average residual values were essentially zero after the first year. The fact that the global temporal trends noted in the residual values did not have a significant effect on the predicted water contents is important. This implies that once the EM measurements are calibrated with a sufficient range of water content values, further calibration points

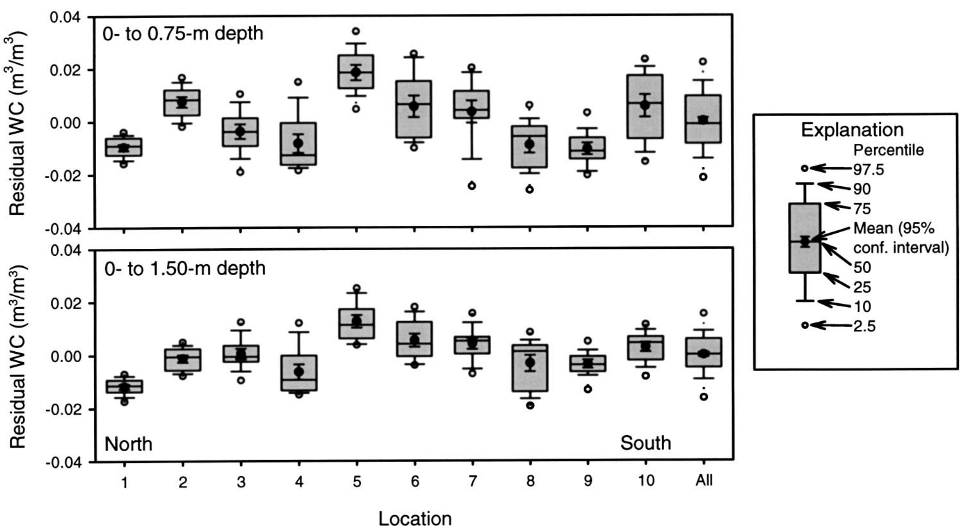

Fig. 8. Percentile box plots of water content residuals for each of the ten monitored locations for the $[\theta_y = a + b(EC_H)]$ models ($n = 350$). Distributions shown for each location are based on 35 residual values. "All" locations represent the pooled values for each depth interval ($n = 350$).

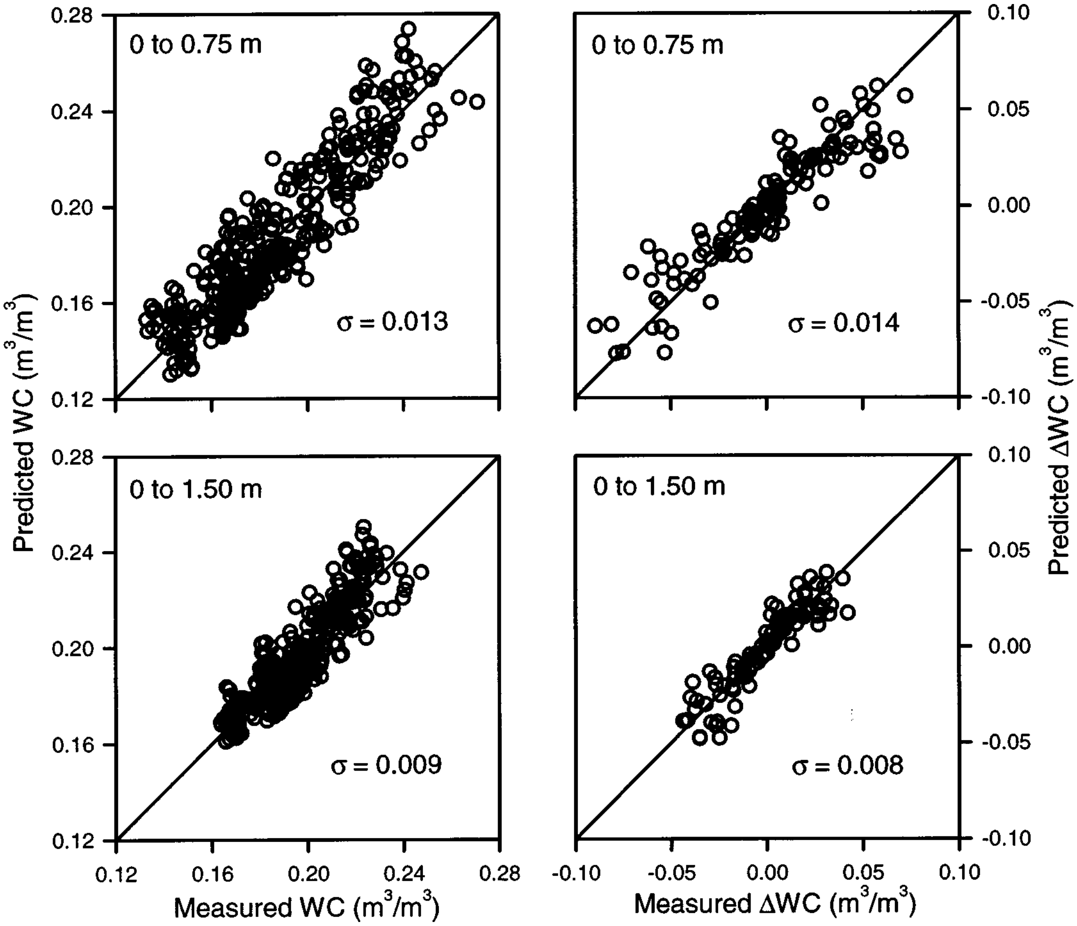

Fig. 10. Comparison between predicted and measured water content (WC) and changes in water content (ΔWC) for the $[\theta_y = a + b(EC_H)]$ models fit to the complete data sets ($n=350$). Lines represent the 1:1 ratio. Water content changes are cumulative over 11 periods when the spatial average was either increasing or decreasing. σ is the standard deviation.

might be limited or eliminated, provided a reasonable assumption about the degree of temporal residual correlation (if any) can be made. For example, one possible approach might be to simply use calibration data acquired from artificially created test plots at different water contents at the beginning of the study. Such a calibration approach would be advantageous because it would limit use of a radioactive source to the initial phase of the study. This result differs, at least for our site, with that of Sheets and Hendrickx (1995), who found it necessary to obtain calibration measurements with the neutron probe for each EM survey in order to obtain the most accurate results.

Alternatively, one could collect periodic water content calibration data at a few preselected sites (as done in this study) in conjunction with a much more detailed EM grid across the survey area. This would represent a more conservative (i.e., safer) approach, because the resulting statistical calibration model could be periodically updated and any temporal (or spatial) residual correlation could be directly modeled. Most importantly, the extra EM data could be used to produce location specific water content predictions (at all nonsampled EM survey sites), more accurate site average estimates, and estimates of either location-specific or site-average changes in water content over time. Such an approach would be quite similar to the EM/salinity calibration techniques advocated by Lesch et al. (1995), except that a temporal component would be incorporated into the calibration approach.

Variability of Estimated Soil Bulk Electrical Conductivity

Estimates of the relative contributions of clay content, salinity, and water content indicate that spatial variability in salinity is the dominant cause of spatial variability in estimated bulk conductivity at our site. Varying salinity alone over the range of measured values resulted in estimated bulk conductivity CV values 3.6 times greater than estimates due to variation in clay content alone and an average of ten times greater than estimates due to variation in water content alone. Varying salinity alone resulted in an average estimated bulk conductivity CV of 7.9% and ranged from 7.8 to 8.0% at different times. Varying clay content alone resulted in an average estimated bulk conductivity CV of 2.2% and remained stable through time. Varying water content alone resulted in an average estimated bulk conductivity CV of 0.8%, and ranged from 0.4 to 1.2% at different times. Therefore, the spatial variability in the predicted water content residual values is predominantly the result of variability in salinity, with clay content variability being of secondary importance at our site. The variability of salinity may be attributed to the heterogeneous nature of the construction source stockpiles. The stockpiled soils were locally derived from deposits at depths ranging from 0 to 10 m. While texturally similar, chloride concentrations varied from ~100 to ~700 mg/kg soil over that depth (Scanlon 2000).

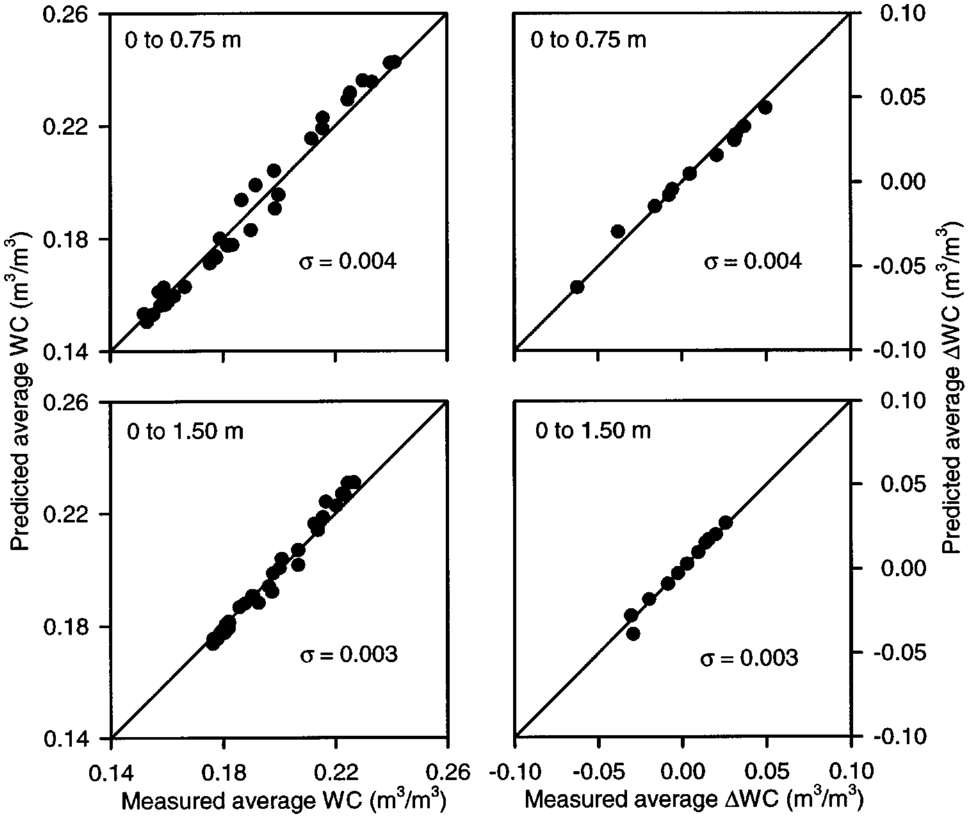

Fig. 11. Comparison between predicted and measured spatially averaged water content (WC) and change in water content (ΔWC) for the $[\theta_y = a + b(EC_H)]$ models fit to the complete data sets ($n=350$). Lines represent the 1:1 ratio. Average water content values for each survey are represented ($n=35$). Average water content changes are cumulative over 11 periods when the spatial average was either increasing or decreasing. σ is the standard deviation.

Predicted Point Location and Spatial Average Water Contents

Monitoring water content and water content changes at point locations provides information regarding engineered cover performance and may aid in identifying areas of potential failure due to focused flow. The ability to rapidly identify such areas can significantly decrease response time to institute corrective action and may help to limit costs through early identification of the problem. Spatially averaged water content or water content change over a given area is generally useful for water-balance calculations and for monitoring overall cover performance.

Because many of the changes in volumetric water content between survey dates at our site were small (<0.01) over the 0- to 0.75-m- and 0- to 1.50-m depth intervals, comparisons between measured and predicted changes in water content using Eq. (5) were generated from the cumulative sums of changes over periods for which the spatial average [Fig. 3(a)] was either increasing or decreasing. Inspection of measured versus predicted values indicates that within the observed range, volumetric water content at individual locations over the 0- to 1.50-m depth interval are predicted with a standard deviation of 0.009 and changes in volumetric water content are predicted with a standard deviation of 0.008 at our site (Fig. 10). The standard deviation values are larger for the 0- to 0.75-m-depth interval with values of 0.013 for volumetric water content and 0.014 for changes volumetric in water content at individual locations. These values are smaller than those of Sheets and Hendrickx (1995), whose overall model for volumetric water content to the 1.50-m depth resulted in a standard deviation of 0.021, which was based on measurements using an EM31 conductivity meter.

In as much as the arithmetic average of the ten water content measurement locations represents the true spatial average at our site, the EC_H models for both depth intervals more accurately predict the spatially averaged water content than water content at individual locations. A comparison of the measured and predicted spatial averages resulted in a standard deviation of 0.003 for both volumetric water content and changes in volumetric water content over the 0- to 1.50-m depth (Fig. 11) with only a slight tendency to overpredict higher water contents. The standard deviation for the 0- to 0.75-m depth was 0.004 for both volumetric water content and changes in volumetric water content, and the model tended to slightly underpredict lower water contents and overpredict higher water contents.

Results from this study compare favorably to those from previous studies that evaluated the use of EM induction for water content monitoring. The range in measured bulk soil electrical conductivity was greater in this study (0.4 to 1.02 dS/m) than in previous studies [0.12 to 0.20 dS/m, Sheets and Hendrickx (1995); 0 to 0.50 dS/m, Kachanoski et al. (1988)]. Volumetric water content could be predicted with greater accuracy in this study (± 0.009) than in previous studies [± 0.02, Sheets and Hendrickx (1995); Kachanoski et al. (1988)]. The accuracy of the electromagnetic induction technique is similar to that of the neutron probe (~ ±0.01) method, with the added advantage of monitoring larger areas more rapidly.

Implications for Water Content Monitoring

In addition to water content, the EM response is influenced by temperature, salinity, and soil texture (clay content). Elevated salinity levels and high clay contents can adversely affect the use of time domain reflectometry (TDR) to monitor water content. Many areas in the western United States have soil conditions that preclude the use of TDR for automated water content monitoring. Elevated salinity levels can actually enhance the EM response through increased sensitivity to both water content and changes in water content. Engineered covers generally are designed to have uniform soil texture and bulk density and as a result are inherently spatially homogeneous. Variations in salinity were not considered during construction of our site and heterogeneity of salinity was found to be the dominant source of soil bulk electrical conductivity spatial variability. Careful attention to salinity and clay content during construction can further limit the heterogeneity of factors that influence the EM response and thereby maximize the potential for using EM to monitor water content. Despite the heterogeneity at our site, EM induction measurements, once standardized for temperature influences, successfully predicted volumetric water content to a depth of 1.50 m to within ±0.009 at point locations and to within ±0.003 of the spatial average calculated from the point location measurements.

The observed water content range and, thus, the simplified linear regression model calibration, required approximately 18 months to establish at our site. Because the model residuals were only slightly correlated with time implies that calibration might have been more rapidly established using test pits having a range of artificially created water contents. This option should be tested.

Conclusions

Water content and changes in water content in the prototype engineered soil cover were accurately predicted using noninvasive electromagnetic induction measurements. The EM38 horizontal dipole mode measurements consistently produced more accurate models than did the vertical dipole mode measurements because most of the water content changes at our site occurred at shallow depths, where the horizontal dipole mode response provided the greatest sensitivity. Models that included only the horizontal dipole mode measurements were better predictors of water content at our site than models that incorporated only the vertical dipole mode measurements. The application of EM induction in this study shows excellent promise for monitoring spatial and temporal variability in water content. Although the particular application discussed in this study is an engineered cover designed for waste containment, this method might also be applied to natural systems, with the understanding that greater variability of salinity and clay content would necessarily lead to less accurate results.

Our results indicate that a simple linear model based on EM induction and neutron probe water content measurements can estimate volumetric water content over the 0- to 1.50-m-depth interval to within ±0.009 at any location ($R^2=0.80$). The spatially averaged volumetric water content could be predicted for the 0- to 1.50-m-depth interval to within ±0.003 ($R^2=0.99$). However, the results of this study are site-specific and unique calibrations would be required at other sites having different soil conditions.

Though statistically significant temporal trends were identified, the trends had little impact on predicted water contents. The lack of a significant temporal impact in the model residuals suggests that calibration of the EM with water content measurements using a neutron probe could be conducted in the initial phases of a study using test pits in natural soils used for cover construction having a range of artificially created water contents, thus limiting the use of a radioactive source. Of course, this approach assumes that both soil salinity and/or clay content remain stable or change only negligibly over time. Conversely, a limited number of neutron probe locations could be used in a study area to facilitate a much more detailed calibration of EM grid data. Such detailed grid data could then be used to produce accurate estimates of the temporally dependent spatial water content pattern, along with a verifiable level of statistical precision. In either scenario, the results of this study demonstrate that EM induction can be used to monitor spatial and temporal variability in water content over large areas.

Acknowledgments

The writers thank Scott Lesch (George E. Brown, Jr., Salinity Laboratory, U.S. Dept. of Agriculture ARS) and James Jennings (Bureau of Economic Geology, Jackson School of Geosciences, The University of Texas at Austin) for their insights and kind assistance with the statistical analysis. Financial support was provided by grants from the U.S. Environmental Protection Agency and the Texas Low-Level Radioactive Waste Disposal Authority. Publication authorized by the Director, Bureau of Economic Geology.

Notation

The following symbols are used in this paper:

°C = degrees centigrade;
C = near-surface neutron probe count correction factor;
EC = bulk soil electrical conductivity;
EC_a = apparent bulk soil electrical conductivity;
EC_e = saturated soil paste extract electrical conductivity;
EC_H = EC_{25} horizontal dipole mode readings;
EC_P = saturated soil paste electrical conductivity;
EC_V = EC_{25} vertical dipole mode readings;
EC_{25} = EC_a standardized to 25°C;
F = ANOCOVA F-test value;
h = separation distance;
n = sample size;
p = ANOCOVA F-test value significance;
R^2 = coefficient of determination;
r = correlation coefficient;
T = temperature;
γ = semivariogram;
θ = volumetric water content;
μ = mean;
σ = standard deviation; and
σ^2 = variance.

References

Anonymous (1954). "Diagnosis and improvement of saline and alkaline soils." *U.S.D.A agricultural handbook 60*, L. A. Richards, ed., U.S. Government Printing Office, Washington, D.C.

Cook, P. G., and Walker, G. R. (1992). "Depth profiles of electrical conductivity from linear combinations of electromagnetic induction

measurements.'' *Soil Sci. Soc. Am. J.,* 56, 1015–1022.
Dalton, F. N. (1992). ''Development of time-domain reflectometry for measuring soil water content and bulk soil electrical conductivity,'' *Advances in measurement of soil physical properties: Bringing theory into practice*, G. C. Topp, W. D. Reynolds, and R. E. Green, eds., Soil Science Society of America, Madison, Wis., 143–167.
Daniel, D. E., and Koerner, R. M., (1995). *Waste containment systems: Guidance for construction, quality assurance, and quality control*, ASCE, New York.
Dwyer, S. F. (2001). ''Finding a better cover.'' *Civ. Eng. (N.Y.)*, 71(1), 58–63.
Fayer, M. J., Rockhold, M. L., and Campbell, M. D. (1992). ''Hydrologic modeling of protective barriers: comparison of field data and simulation results.'' *Soil Sci. Soc. Am. J.,* 56, 690–700.
Gardner, W. H. (1986). ''Water content'' *Methods of soil analysis, Part 1, Physical and mineralogical methods*, A. Klute, ed., Monograph 9, American Society of Agronomy, Madison, Wis., 493–545.
Grant, D. R. (1975). ''Measurement of soil moisture near the surface using a moisture meter.'' *J. Soil Sci.,* 26, 124–129.
Greacen, E. L., Correll, R. L., Cunningham, R. B., Johns, G. G., and Nicholls, D. (1981). ''Calibration,'' *Soil water assessment by the neutron method*, E. L. Greacen, ed., CSIRO, Adelaide, Australia.
Kachanoski, R. G., De Jong, E., and Van Wesenbeeck, I. J. (1990). ''Field scale patterns of soil water storage from non-contacting measurements of bulk electrical conductivity.'' *Can. J. Soil Sci.,* 70, 537–541.
Kachanoski, R. G., Gregorich, E. G., and Van Wesenbeeck, I. J. (1988). ''Estimating spatial variations of soil water content using noncontacting electromagnetic inductive methods.'' *Can. J. Soil Sci.,* 68, 715–722.
Khire, M. V., Benson, C. H., and Bosscher, P. J. (1997). ''Water balance modeling of earthen final covers.'' *J. Geotech. Geoenviron. Eng.,* 123(8), 744–754.
Lesch, S. M., Strauss, D. J., and Rhoades, J. D. (1995). ''Spatial prediction of soil salinity using electromagnetic induction techniques. I. Statistical prediction models: A comparison of multiple linear regression and cokriging.'' *Water Resour. Res.,* 31, 373–386.
McKenzie, R. C., Chomistek, W., and Clark, N. F. (1989). ''Conversion of electromagnetic inductance readings to saturated paste extract values in soils for different temperature, texture, and moisture conditions.'' *Can. J. Soil Sci.,* 69, 25–32.
McNeill, J. D. (1980). ''Electromagnetic terrain conductivity measurement at low induction numbers.'' *Technical Note TN-6, Geonics Ltd.*, Mississauga, Ont.
Paine, J. G., Goldsmith, R. S., and Scanlon, B. R. (1998). ''Electrical conductivity and gamma-ray response to clay, water, and chloride content in fissured sediments, Trans-Pecos Texas.'' *Environ. Eng. Geosci.,* 4, 225–239.
Pannatier, Y. (1996). *Variowin software for spatial data analysis in 2D*, Springer-Verlag, New York.
Rhoades, J. D. (1992). ''Instrumental field methods of salinity appraisal.'' *Advances in measurement of soil physical properties: Bringing theory into practice*, G. C. Topp, W. D. Reynolds, and R. E. Green, eds., *Soil Science Society of America, Special Pub. No. 30*, Madison, Wis., 231–248.
Rhoades, J. D., Shouse, P. J., Alves, W. L., Manteghi, N. A., and Lesch, S. M. (1990). ''Determining soil salinity from soil electrical conductivity using different models and estimates.'' *Soil Sci. Soc. Am. J.,* 54, 46–54.
Scanlon, B. R. (2000). ''Uncertainties in estimating water fluxes and residence times using environmental tracers in an arid unsaturated zone.'' *Water Resour. Res.,* 36, 395–409.
Scanlon, B. R., Christman, M., Reedy, R. C., Gross, B., Simunek, J., and Porro, I. (2003). ''Intercode comparisons for simulating water balance of surficial sediments in semiarid regions.'' *Water Resour. Res.*, in press.
Scanlon, B. R., Paine, J. G., and Goldsmith, R. S. (1999). ''Evaluation of electromagnetic induction as a reconnaissance technique to characterize unsaturated flow in an arid setting.'' *Ground Water,* 37, 296–304.
Sheets, K. R., and Hendrickx, J. M. H. (1995). ''Noninvasive soil water content measurement using electromagnetic induction.'' *Water Resour. Res.,* 31, 2401–2409.
Snedecor, G. W., and Cochran, W. G., (1967). *Statistical methods,* 6th Ed., The Iowa State Univ. Press, Ames, Iowa.
Ward, A. L., and Gee, G. W. (1997). ''Performance of a field-scale surface barrier.'' *J. Environ. Qual.,* 26, 694–705.
Wing, N. R., and Gee, G. W. (1994). ''Quest for the perfect cap.'' *Civ. Eng. (N.Y.),* 64(10), 38–41.